Thermodynamic and in Vitro Replication Studies of an Intrastrand G[8-5]C Cross-Link Lesion†

Chunang Gu‡ and Yinsheng Wang*,§

Environmental Toxicology Graduate Program and Department of Chemistry-027, University of California, Riverside, California 92521-0403

Received January 7, 2005; Revised Manuscript Received March 26, 2005

ABSTRACT: We recently identified, from the γ-irradiation mixture of duplex DNA, a new intrastrand G[8-5]C cross-link lesion, in which the C8 atom of guanine and the C5 atom of its 3′ neighboring cytosine are covalently bonded, and carried out in vitro replication studies for the lesion-bearing substrate with a translesion synthesis polymerase, yeast polymerase η. Here we extended the in vitro replication studies to two replicative polymerases, exonuclease-deficient bacteriophage T7 DNA polymerase (T7$^-$) and HIV reverse transcriptase (HIV-RT). Primer extension assays showed that both polymerases stopped synthesis after incorporating a nucleotide opposite the 3′-cytosine in the G[8-5]C lesion. Steady-state kinetic measurements for nucleotide incorporation opposite the 3′-cytosine of the lesion showed that both T7$^-$ and HIV-RT preferentially incorporated the correct nucleotide, dGMP. We also examined the thermal stabilities and base pairing properties of G[8-5]C in d(ATGGCG[8-5]CGCTAT). The G[8-5]C lesion destabilizes the duplex form by approximately 4 kcal/mol in free energy at 25 °C relative to the undamaged parent duplex, and the thermally most stable duplex has natural bases opposite the lesion.

Reactive oxygen species (ROS) can be produced by a number of endogenous and exogenous pathways (*1*). ROS can cause damage to DNA, and a multitude of lesions with modifications on a single nucleobase have been found (*2*). In addition to those single-nucleobase lesions, Box, Cadet, their co-workers, and we (*3*−*16*) have identified the structures of several oxidative intrastrand cross-link lesions. In this respect, we found that γ-irradiation of a synthetic duplex oligodeoxyribonucleotide (ODN)[1] can give rise to an intrastrand G[8-5]C cross-link in which the C8 atom of guanine and the C5 atom of its neighboring 3′-cytosine are covalently bonded (*13*). The lesion was proposed to arise from the dehydration of the coupling product between guanine and the 6-hydroxy-5,6-dihydrocytosin-5-yl radical, which is a secondary radical arising from attack of the hydroxyl radical (•OH) on the C6 atom of cytosine (*6*) (Figure 1).

DNA lesions are present in replicating DNA if they are not repaired in time; the ability of DNA polymerases to insert appropriate nucleotide(s) opposite those lesions is important for maintaining genomic integrity (*17*−*19*). In addition, some DNA lesions can cause stalling of DNA polymerases, which may lead to cell death (*17*). In vitro replication studies of DNA lesions with purified DNA polymerases can allow us to examine the extent to which the lesions can block replication and to investigate the mutagenic properties of the lesions (*17*).

From the point of view of structure, the oxidative intrastrand cross-link lesions are similar to DNA photoproducts, including the *cis*-*syn*-cyclobutane dimer and the (6-4)pyrimidine-pyrimidone product at the TT site, i.e., T[*c*,*s*]T and T(6-4)T, respectively, for which extensive in vitro replication studies have been carried out. In this regard, most replicative DNA polymerases, such as the Klenow fragment of *Escherichia coli* DNA polymerase I and T7 DNA polymerase, belong to the high-fidelity Pol A family (*20*), and they have constrained active sites. It has been proposed that T7 DNA polymerase inserts a dAMP opposite the 3′-T of T[*c*,*s*]T with the photoproduct lying outside of the active site, whereas the incoporation of nucleotide opposite the 5′-T takes place while the photoproduct stays in the active site (*21*−*23*).

Many "Y" superfamily polymerases are involved in translesion synthesis, which allows DNA replication to proceed past lesions and prevents acute cell death arising from replication block (*24*, *25*). Among these polymerases, eukaryotic DNA polymerase η, which is the gene product of Rad30 in budding yeast *Saccharomyces cerevisiae* (*26*) and the variant form of *xeroderma pigmentosum* (XP-V) in humans (*27*), has been extensively studied. Yeast and human pol η can efficiently bypass T[*c*,*s*]T in an error-free manner (*26*, *28*). On the other hand, pol η cannot bypass a T(6-4)T, and it inserts a dGMP opposite the 3′-T of the lesion (*29*).

In an earlier study (*13*), we found that several polymerases cannot bypass the G[8-5]C lesion efficiently. Except for yeast

† This work was supported by the National Institutes of Health (Grant R01 CA96906).

* To whom correspondence should be addressed: Department of Chemistry-027, University of California, Riverside, CA 92521-0403. Telephone: (951) 827-2700. Fax: (951) 827-4713. E-mail: yinsheng.wang@ucr.edu.

‡ Environmental Toxicology Graduate Program.

§ Department of Chemistry.

[1] Abbreviations: PAGE, polyacrylamide gel electrophoresis; XP-V, variant form of *xeroderma pigmentosum*; T[*c*,*s*]T, *cis*,*syn*-cyclobutane pyrimidine dimer at the TT site; T[6-4]T, (6-4) pyrimidine-pyrimidone product at the TT site; ODN, oligodeoxyribonucleotide; T7$^-$, exonuclease-deficient T7 DNA polymerase; HIV-RT, human immunodeficiency virus reverse transcriptase; T_m, melting temperature.

10.1021/bi050036+ CCC: $30.25
Published on Web 05/27/2005

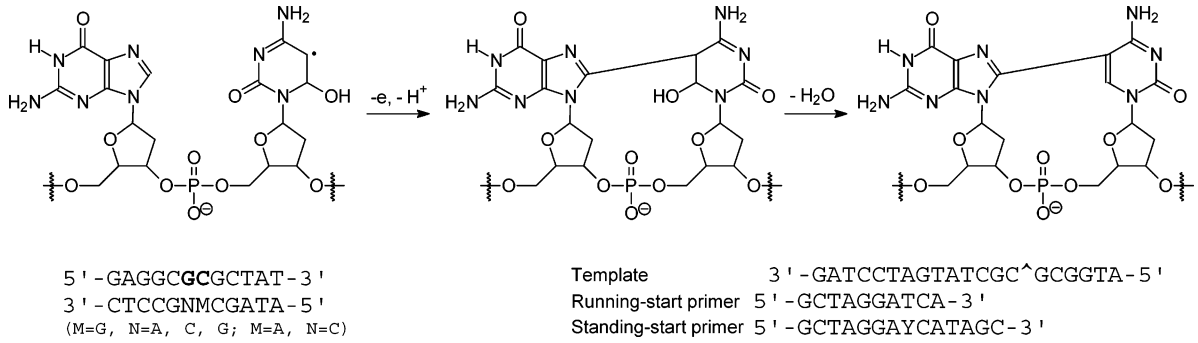

FIGURE 1: (Top) Formation of G[8-5]C from hydroxyl radical attack. (Bottom) Substrates used for melting temperature measurements (left) and substrates employed for in vitro replication studies (right).

pol η, which has been shown to be able to replicate through T[*c*,*s*]T efficiently and accurately (*26*, *28*), other polymerases stop synthesis after having incorporated a nucleotide opposite the 3′-C of G[8-5]C. In addition, pol η inserts the correct nucleotide, dGMP, opposite the 3′-C of G[8-5]C at an efficiency similar to that of the insertion of dGMP opposite the cytosine in the control undamaged substrate. Incoporation opposite the 5′-G in the leison, however, is error-prone, and purine nucleotides are preferentially inserted (*13*).

In this paper, we extended the steady-state kinetic measurements to two replicative DNA polymerases, exonuclease-deficient T7 DNA polymerase (T7$^-$) and HIV reverse transcriptase (HIV-RT). We also examined the influences of G[8-5]C on the thermal stability and base pairing properties of DNA duplexes.

EXPERIMENTAL PROCEDURES

All oligodeoxyribonucleotides (ODNs) used in this study were purchased from Integrated DNA Technologies (Coraville, IA). [γ-^{32}P]ATP was obtained from Amersham Biosciences Co. (Piscataway, NJ). All other chemicals unless otherwise noted were obtained from Sigma-Aldrich (St. Louis, MO). The double mutant form (D5A/E7A) of T7$^-$ (*30*, *31*) and its processivity factor, thioredoxin, were kindly provided by J.-S. A. Taylor at Washington University (St. Louis, MO). HIV-RT was a kind gift from J. Termini at the City of Hope National Medical Center (Duarte, CA), and its purification was reported previously (*32*). The purities for these two polymerases are >90%.

Preparation of an ODN Substrate Containing G[8-5]C for in Vitro Replication Studies. The G[8-5]C-containing ODN for in vitro replication studies was prepared as described in a previous paper (*13*). The dodecameric lesion-bearing substrate d(ATGGCG[8-5]CGCTAT) was obtained from UV irradiation of a 5-bromocytosine-containing duplex DNA (*12*), and it was ligated with the 5′-phosphorylated d(GATCCTAG) in the presence of a template ODN, d(CCGCTCCCTAGGATCATAGCGCGCCAT), by using previously described procedures (*13*). The desired lesion-containing 20-mer ODN was purified by 20% denaturing polyacrylamide gel electrophoresis (PAGE) and desalted by using an NAP-25 Column (Amersham Bioscience Co.). The purity of the product was further confirmed by PAGE analysis (data not shown).

For primer extension under standing-start conditions, the 20-mer lesion-containing template or normal template (20 nM) with a GC pair in lieu of the G[8-5]C cross-link was annealed with a 5′-^{32}P-labeled 14-mer primer (10 nM, Figure 1); to the duplex mixture were added individual dNTPs or a mixture of all four dNTPs as well as a DNA polymerase. The reaction was carried out at 37 °C in a buffer containing 10 mM Tris-HCl (pH 7.5), 5 mM $MgCl_2$, and 7.5 mM DTT for 60 min or for another time period as indicated. The concentrations of polymerases that were used appear in the figures, and 100-fold more (in moles) thioredoxin from *E. coli* was added to the T7$^-$-induced extension reaction mixtures. The reaction was terminated by adding a 2 volume excess of formamide gel-loading buffer [80% formamide, 10 mM EDTA (pH 8.0), 1 mg/mL xylene cyanol, and 1 mg/mL bromophenol blue]. Primer extension under running-start conditions was carried out in a similar fashion except that a shorter primer, d(GCTAGGATCA), was used (Figure 1). The products were resolved on 20% (1:19) cross-linked denaturing polyacrylamide gels containing 8 M urea. Gel band intensities of the substrates and products were quantified by using a Typhoon 9410 Variable Mode Imager (Amersham Biosciences Co.) and ImageQuant version 5.2 (Amersham Biosciences Co.).

Steady-State Kinetic Measurements. We followed the previously described procedure (*33*, *34*) for the steady-state kinetic analyses. In this measurement, the primer−template complex (10 nM) was incubated with either T7$^-$ (2 nM) or HIV-RT (0.3 μM) in the presence of an individual dNTP at various concentrations. The reaction was carried out at room temperature with the same reaction buffer as described for the primer extension experiments. The dNTP concentration and reaction time (10−60 min) were optimized for different insertion reactions to allow for less than 20% primer extension (*34*). The V_{obs}, or the observed rate of dNTP incorporation, was plotted as a function of dNTP concentration, and the apparent K_m and V_{max} steady-state kinetic parameters for the incorporation of both correct and incorrect nucleotides were determined by fitting the data with the Michaelis−Menten equation:

$$V_{obs} = \frac{V_{max}[\text{dNTP}]}{K_m + [\text{dNTP}]}$$

The efficiency of nucleotide incorporation was determined by the V_{max}/K_m ratio. The fidelity of nucleotide incorporation was then calculated by the frequency of misincorporation (f_{inc}) with the following equation:

$$f_{inc} = \frac{(V_{max}/K_m)_{incorrect}}{(V_{max}/K_m)_{correct}}$$

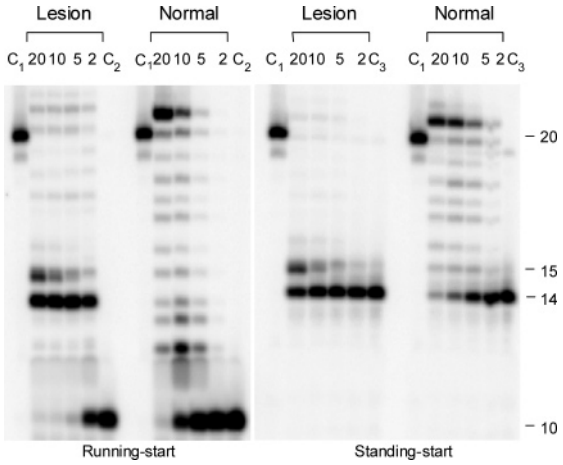

FIGURE 2: Primer extension assays for a G[8-5]C-bearing substrate and its control undamaged substrate with T7$^-$: left, running-start experiments in which 5′-^{32}P-labeled d(GCTAGGATCA) was used as the primer; and right, standing-start experiments in which 5′-^{32}P-labeled d(GCTAGGATCATAGC) was used as the primer. T7$^-$ at the indicated concentrations was incubated with 10 nM substrate and 100 mM dNTPs at room temperature for 60 min. Controls are as follows: C_1, full-length 20-mer product; C_2, running-start primer; and C_3, standing-start primer.

Measurement of Melting Curves. The above 12-mer G[8-5]C-containing ODN was employed for melting temperature measurements. It was annealed with another 12-mer ODN to form the duplex. The specific nucleotide sequences are as follows: strand 1, 5′-ATGGCXYGCTAT-3′; and strand 2, 3′-TACCGNMCGATA-5′. X and Y represent the parental GC pair and its [8-5] cross-link lesion, and M and N denote two of the four standard nucleotides, A, C, G, and T (Figure 1). We refer to the duplexes by abbreviations of the form strand 1·strand 2, where only nucleobases X and Y or M and N of each strand are listed and both of them are in the 5′ to 3′ sequence order.

UV absorbance versus temperature profiles were recorded on a Varian Cary 500 spectrophotometer (Varian Inc., Palo Alto, CA), and the ODNs were dispersed in a 1.0 mL solution containing 250 mM NaCl, 10 mM sodium cacodylate, and 0.1 mM EDTA (pH 7.0) at a total ODN concentration (C_t) of 2.0, 3.4, 5.6, 9.5, or 16 μM. The absorbance was recorded in the reverse and forward directions for a temperature range of 80−10 °C at a rate of 1 °C/min, and the melting temperature (T_m) value was obtained by the derivative method.

The thermodynamic parameters were obtained from the van't Hoff plot (*35*), where the reciprocal of T_m was plotted against ln(C_t/4):

$$\frac{1}{T_m} = \left(\frac{R}{\Delta H^\circ}\right) \ln\frac{C_t}{4} + \frac{\Delta S^\circ}{\Delta H^\circ}$$

and

$$\Delta G^\circ = \Delta H^\circ - T\Delta S^\circ$$

where R is the gas constant (1.987 cal mol^{-1} K^{-1}). The error limits for ΔG°, ΔH°, and ΔS° derived from fitted parameters were calculated by using previously described equations (*36*, *37*).

RESULTS

In Vitro Replication Studies with T7$^-$ and HIV-RT. We examined the mutagenic properties of G[8-5]C by carrying out primer extension assays with two replicative polymerases, T7$^-$ and HIV-RT. We chose these two polymerases because they have been extensively used as model replicative polymerases and the major mammalian leading-strand polymerase pol δ exhibits behavior similar to that of T7$^-$ and HIV-RT in kinetic studies (*38*, *39*). Together with previous studies of translesion synthesis polymerase, yeast pol η, the investigations on the action of replicative polymerases (T7$^-$ and HIV-RT) on the G[8-5]C cross-link can offer further insights into the mutagenic properties of the lesion.

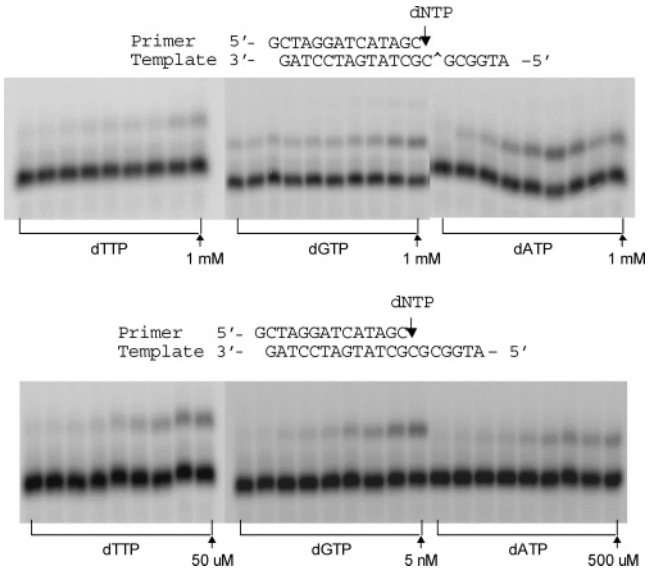

FIGURE 3: Steady-state kinetic measurements for incorporation of dAMP, dGMP, and dTMP opposite the cytosine portion of G[8-5]C (top) or the cytosine at an undamaged GC site (bottom). T7$^-$ (2 nM) was incubated with 10 nM DNA substrate at room temperature for 10 min. The highest dNTP concentration is shown in the figure, and the concentration ratio of dNTP between adjacent lanes was 0.6.

A 20-mer lesion-containing substrate was used as a template, and it was constructed by ligating d(ATGGCG-[8-5]CGCTAT) with a 5′-phosphorylated 8-mer ODN as described in Experimental Procedures. Primer extension assays with T7$^-$ under both standing- and running-start conditions show that, in the presence of all four dNTPs, the synthesis stops mostly after the incorporation of the first nucleotide opposite the 3′-C of the lesion, though a very small percentage of bypass product can also be detected (Figure 2). For this reason, the following steady-state kinetic parameters were only determined for nucleotide insertion opposite the 3′-C of the G[8-5]C lesion. The product from the replication of the undamaged template is one or two nucleotides longer than the expected full-length product (21-mer, Figures 1 and 2), indicating that blunt-end addition occurred (*40*, *41*).

We next determined the steady-state kinetic parameters for nucleotide incorporation opposite the 3′-C of the G[8-5]C lesion and the undamaged bases in the control substrate by T7$^-$ (Figure 3) (Michaelis−Menten plots for one set of measurements are shown in the Supporting Information). The results showed that the insertion of the correct nucleotide, dGMP, opposite the 3′-C of the undamaged substrate is significantly more efficient than those of the other three nucleotides (Table 1).

When the data for the damaged and the undamaged substrates are compared (Table 1), the efficiency for incor-

Table 1: Fidelity of Nucleotide Incorporation by T7$^-$ on the Undamaged Substrate and a G[8-5]C-Containing Substrate (Figure 1) As Determined by Steady-State Kinetic Measurements (K_m and V_{max} are average values based on three independent measurements)

dNTP	V_{max} (nM/min)	K_m (μM)	V_{max}/K_m	f_{inc}
Undamaged Substrate, 14-mer Primer (5′-GCTAGGATCATAGC-3′)				
dATP	0.23 ± 0.02	110 ± 20	2.1×10^{-3}	3.0×10^{-5}
dGTP	0.48 ± 0.07	0.0066 ± 0.0006	72	1
dCTP	ND[a]	ND[a]	N/A[b]	N/A[b]
dTTP	0.25 ± 0.02	27 ± 4	9.2×10^{-3}	1.3×10^{-4}
Damaged Substrate, 14-mer Primer				
dATP	0.087 ± 0.011	280 ± 40	3.0×10^{-4}	0.38
dGTP	0.011 ± 0.0004	14 ± 2	8.0×10^{-4}	1
dCTP	ND[a]	ND[a]	N/A[b]	N/A[b]
dTTP	0.0038 ± 0.0006	170 ± 30	2.3×10^{-5}	2.8×10^{-2}

[a] Below detection limits. [b] Not available.

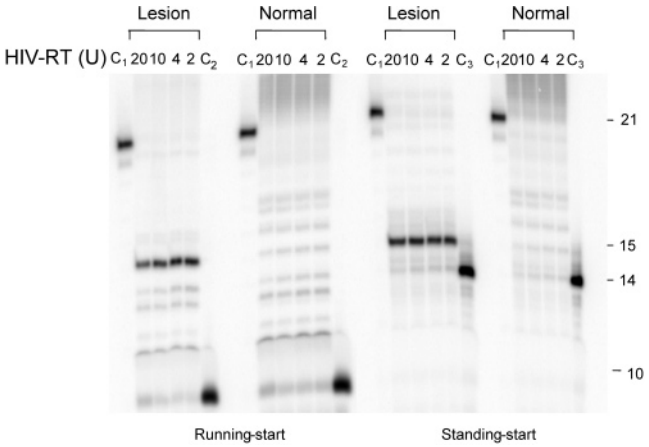

FIGURE 4: Primer extension assays for incorporation of a nucleotide opposite a G[8-5]C-bearing substrate and its control undamaged substrate with HIV-RT (1 unit = 1.89 pmol): left, running-start experiments in which 5′-^{32}P-labeled d(GCTAGGATCA) was used as the primer; and right, standing-start experiments in which 5′-^{32}P-labeled d(GCTAGGATCATAGC) was used as the primer. HIV-RT at the indicated concentrations was incubated with 10 nM substrate and 100 mM dNTPs at room temperature for 60 min. Controls are as follows: C_1, full-length 20-mer product; C_2, running-start primer; and C_3, standing-start primer.

Table 2: Fidelity of Nucleotide Incorporation by HIV-RT on the Undamaged Substrate and a G[8-5]C-Containing Substrate (Figure 1) As Determined by Steady-State Kinetic Measurements (K_m and V_{max} are average values based on three independent measurements)

dNTP	V_{max} (nM/min)	K_m (μM)	V_{max}/K_m	f_{inc}
Undamaged Substrate, 14-mer Primer (5′-GCTAGGATCATAGC-3′)				
dATP	0.074 ± 0.003	90 ± 10	8.2×10^{-4}	1.6×10^{-5}
dGTP	0.72 ± 0.06	0.014 ± 0.002	50	1
dCTP	ND[a]	ND[a]	N/A[b]	N/A[b]
dTTP	0.70 ± 0.05	60 ± 7	1.2×10^{-2}	2.3×10^{-4}
Damaged Substrate, 14-mer Primer				
dATP	0.0023 ± 0.0001	21 ± 4	1.1×10^{-4}	7.3×10^{-4}
dGTP	0.014 ± 0.001	0.077 ± 0.011	0.19	1
dCTP	ND[a]	ND[a]	N/A[b]	N/A[b]
dTTP	0.0061 ± 0.0003	9.5 ± 1.7	6.4×10^{-4}	3.6×10^{-3}

[a] Below detection limits. [b] Not available.

porating dGMP opposite the 3′-C is markedly reduced (by $\sim 10^5$ times) by the presence of the lesion. The substitution of the unmodified GC dinucleotide with G[8-5]C also causes the efficiency for the corresponding incorporation of dAMP to decrease by approximately 10-fold. The correct nucleotide, dGMP, is still inserted ~3-fold as efficiently as dAMP, which is in turn preferred by approximately 14 times over the insertion of dTMP (Table 1). The insertion of dCMP is not detectable in the presence of either the damaged or undamaged templates. The above steady-state kinetic measurements, therefore, demonstrate that the efficiencies for nucleotide incorporation are significantly decreased by the presence of the G[8-5]C cross-link lesion. The fidelity of the nucleotide incorporation, however, is not drastically reduced.

It's worth noting that the velocity versus dGTP concentration plot for the damaged substrate deviates from the typical parabolic curve when the concentrations of dGTP are higher than ~200 μM (data not shown). The reason for observing this biphasic kinetic behavior is unclear. However, the data points with dGTP concentrations of ≤ 120 μM, which fit into a parabolic curve, were used for deriving the Michaelis−Menten kinetic parameters (Figure S2 of the Supporting Information).

Like T7$^-$, HIV-RT stops synthesis mostly after the incorporation of the first nucleotide opposite the 3′-C of the lesion (Figure 4). We then determined the steady-state kinetic parameters for nucleotide insertions opposite the 3′-C of the cross-link lesion or opposite the cytosine of the control undamaged substrate (Figure 5 and Table 2; Michaelis−Menten plots for one set of measurements are shown in Figure S4 of the Supporting Information). We observed that the kinetic curve for dGTP insertion opposite the 3′-C of the cross-link lesion by HIV-RT is biphasic, similar to what we found for T7$^-$ (Figure S4 of the Supporting Information). Again, the kinetic data in the low concentration range were employed for determining K_m and V_{max}.

When the data for the lesion-containing and undamaged substrates are compared, the efficiency for dGMP incorporation opposite the 3′-C is reduced by 2 orders of magnitude with the presence of the lesion, whereas the efficiency for the respective incorporation of dAMP only decreases by less than 10-fold (Table 2). Nevertheless, dGMP is still the most favorite nucleotide being inserted opposite the 3′-C of the cross-link lesion, followed by dTMP and dAMP, which are approximately 300 and 1400 times less frequently inserted, respectively, than dGMP (insertion of dCMP is again undetectable). Therefore, during the replication by HIV-RT, the presence of the G[8-5]C cross-link decreases significantly the efficiency, but not the fidelity, of nucleotide incorporation opposite the 3′-C.

Thermodynamic Properties of DNA Duplexes Containing G[8-5]C. The dodecameric ODNs containing either normal GC bases or G[8-5]C described in the Experimental Procedures were used for the thermodynamic analysis (Figure 1). Thermal curves, which monitored the UV absorbance at $\lambda = 260$ nm as a function of temperature, were measured at total ODN concentrations (C_t) varying from 2.0 to 16.0 μM. Thermodynamic parameters for each duplex were determined from the T_m data by the van't Hoff method, assuming a two-state (all-or-none) model for duplex melting, i.e., the double-helical state or in the "random coil" state (*35*). In this context, we determined $\Delta H°$ and $\Delta S°$ by fitting T_m^{-1} versus $\ln(C_t/4)$ [the T_m^{-1} vs $\ln(C_t/4)$ plots for lesion-bearing duplexes are shown in Figure 6, and the corresponding plots for unmodified substrates are shown in the Supporting Information]. The $\Delta G°$ values for duplex formation were calculated from the $\Delta H°$ and $\Delta S°$ values with the understanding that $\Delta G°$ values calculated for temperatures far from the melting

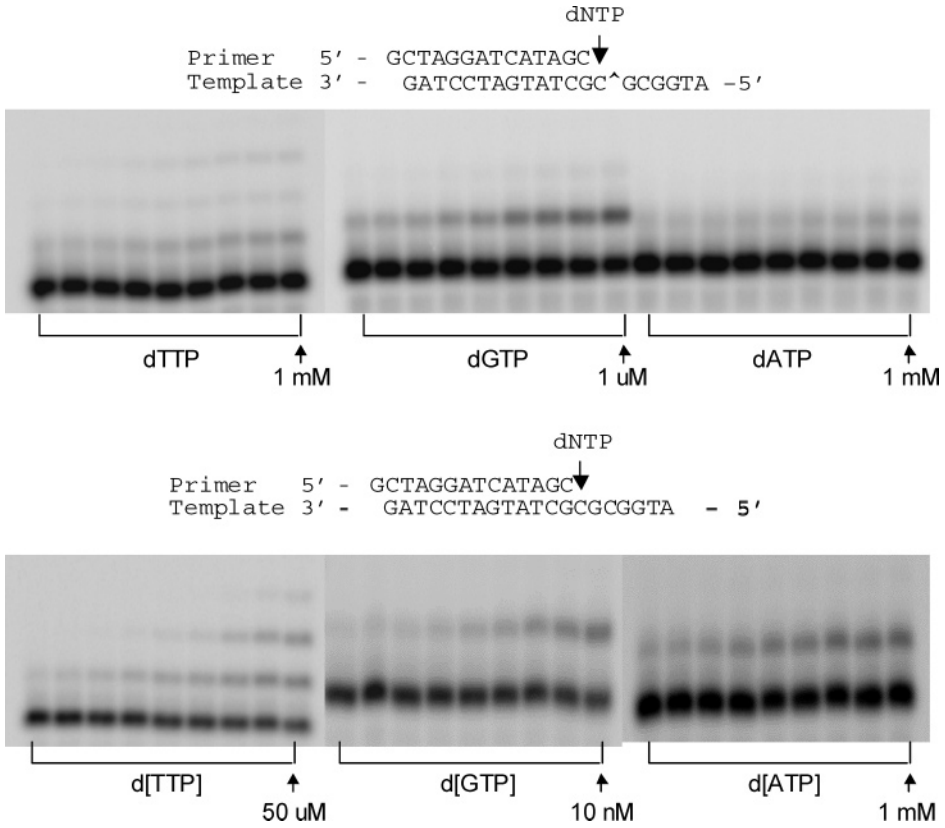

FIGURE 5: Steady-state kinetic measurements for incorporation of dAMP, dGMP, and dTMP opposite the cytosine portion of G[8-5]C (top) or the cytosine at an undamaged GC site (bottom). HIV-RT (4 units, 1 unit = 1.89 pmol) was incubated with 10 nM DNA substrate at room temperature for 10 min. The highest dNTP concentration is shown in the figure, and the concentration ratio of dNTP between adjacent lanes was 0.6.

Table 3: Thermodynamic Parameters of Duplex Formation in a 250 mM NaCl Solution

duplex	T_m[a] (°C)	ΔT_m[b] (°C)	ΔH (kcal/mol)	ΔS (cal mol^{-1} K^{-1})	$\Delta G_{25\,°C}$ (kcal/mol)	$\Delta\Delta G_{25\,°C}$ [c] (kcal/mol)
5′-ATGGCGCGCTAT-3′						
3′-TACCGYXCGATA-5′						
X = G, Y = C (GC·GC)	60.0		−77.6 ± 3.7	−204 ± 11	−14.34 ± 0.29	
X = G, Y = G (GC·GG)	49.0		−80.2 ± 4.1	−220 ± 13	−11.83 ± 0.22	
X = G, Y = A (GC·GA)	47.0		−70.2 ± 1.7	−190 ± 5	−11.13 ± 0.05	
X = A, Y = C (GC·AC)	41.0		−77.1 ± 0.3	−217 ± 1	−9.92 ± 0.01	
5′-ATGGCG[8-5]CGCTAT-3′						
3′-TACCGY XCGATA-5′						
X = G, Y = C (G[8-5]C·GC)	42.5	17.5	−83.6 ± 2.3	−236 ± 7	−10.34 ± 0.06	4.00 ± 0.35
X = G, Y = G (G[8-5]C·GG)	32.5	16.5	−70.2 ± 1.0	−201 ± 3	−7.90 ± 0.02	3.93 ± 0.24
X = G, Y = A (G[8-5]C·GA)	34.5	12.5	−66.5 ± 3.2	−187 ± 10	−8.43 ± 0.02	2.70 ± 0.07
X = A, Y = C (G[8-5]C·AC)	20.0	21.0	−33.0 ± 1.2	−84 ± 4	−7.05 ± 0.06	2.87 ± 0.07

[a] $C_t = 2.0\ \mu$M. [b] $\Delta T_m = T_m$(parent duplex) − T_m(lesion-containing duplex). [c] $\Delta\Delta G_{25\,°C} = \Delta G_{25\,°C}$(lesion-containing duplex) − $\Delta G_{25\,°C}$(undamaged duplex).

temperatures may not be accurate (*42*). The thermodynamic parameters, as well as the T_m values when $C_t = 2.0\ \mu$M, are listed in Table 3.

From the data listed in Table 3, it is quite clear that the replacement of the GC pair with G[8-5]C results in a decrease in the thermal stability of the duplex by ~4 kcal/mol in free energy at 25 °C ($\Delta G°$ values of −10.34 and −14.34 kcal/mol for the formation of G[8-5]C·GC and GC·GC, respectively). The duplex destabilization caused by the lesion is comparable in magnitude to that induced by one mismatched base pair in the same sequence context, which results in an increase in $\Delta G°$ ranging from 2.5 to 4.4 kcal/mol (Table 3).

To examine the base pairing properties of G[8-5]C, we also determined the thermodynamic parameters for the formation of duplexes with mutated bases opposing the lesion, i.e., compound lesions. It turned out that the duplex with G opposite the 3′-C of G[8-5]C is more stable than the corresponding duplex with A by 3.3 kcal/mol. In addition, a C opposing the 5′-G of the cross-link lesion is preferred over G and A by 2.4 and 1.9 kcal/mol, respectively. Therefore, among the duplex sequences that we examined, the most stable duplex has natural bases opposite the lesion.

DISCUSSION

Previous work from this laboratory demonstrated that the intrastrand cross-link lesion, G[8-5]C, can be induced in duplex DNA by γ-irradiation (*13*). This lesion is structurally analogous to dimeric DNA photoproducts, the cisplatin−GG adduct, and other intrastrand cross-link lesions. In vitro replication studies showed that the two replicative poly-

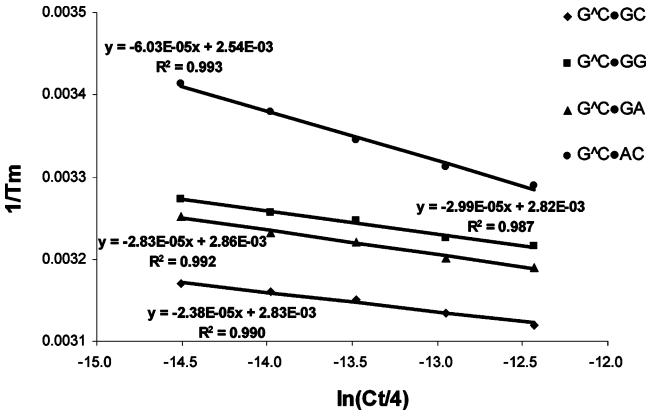

FIGURE 6: Plots of $1/T_m$ vs $\ln(C_t/4)$ for the duplexes containing a G[8-5]C intrastrand cross-link lesion. The duplex is d(ATGGCXYGCTAT)·d(ATAGCMNGCCAT), where XY·MN represents G^C·GC (◆), G^C·GG (■), G^C·GA (▲), and G^C·AC (●) (G^C is G[8-5]C).

merases, i.e., T7$^-$ and HIV-RT, stop synthesis mostly after having inserted the first nucleotide opposite the 3′-C of the lesion.

Steady-state kinetic measurements for nucleotide incorporation showed that both T7$^-$ and HIV-RT insert the correct base, dGMP, opposite the 3′-C of the G[8-5]C lesion. T7$^-$ belongs to the high-fidelity pol A family of DNA polymerases, which adopt constrained active sites (*20*, *43*). Compared with the synthesis opposite the 3′-T of T[*c*,*s*]T by T7$^-$ (*21*, *22*), the preference for insertion of dGMP over dAMP opposite the 3′-C suggests that, even with the constrained active site of the polymerase, the hydrogen bonding properties of the 3′-C of G[8-5]C might be conferred during nucleotide incorporation by T7$^-$. Likewise, HIV-RT also inserts the correct nucleotide, i.e., dGMP, opposite the 3′-C more preferentially than dAMP and dTMP by approximately 300- and 1400-fold, respectively. Therefore, like we observed with yeast pol η (*13*), the fidelities of nucleotide insertion opposite the 3′-C by T7$^-$ and HIV-RT are not appreciably compromised by the presence of the lesion. In a manner different from that of pol η, which can bypass the lesion, T7$^-$ and HIV-RT stop synthesis mostly after incorporating the first correct nucleotide.

The $\Delta G°$ for duplex formation determined from the melting curves showed that the presence of a G[8-5]C cross-link causes an increase in $\Delta G°$ at 25 °C of approximately 4.0 kcal/mol relative to that of the parent duplex. The destabilization caused by the intrastrand cross-link lesion is similar to those reported for similar-length duplexes containing a single-nucleobase lesion. For instance, the presence of 8-oxo-2′-deoxyguanosine (*42*) and the thymine glycol (*44*) destabilizes the duplex DNA by 3.4 and 4.7 kcal/mol, respectively. Compared with that of the structurally related TT DNA photoproducts, the destabilization caused by G[8-5]C is greater than that with T[*c*,*s*]T ($\Delta\Delta G = 1.5$ kcal/mol) but less than that with (6-4) and Dewar TT photoproducts ($\Delta\Delta G \approx 6$ kcal/mol) (*45*). Therefore, we may infer that G[8-5]C induces more significant structural distortion in double-stranded DNA than T[*c*,*s*]T, but less than (6-4) and Dewar TT photoproducts.

The instability of duplex DNA induced by the lesion may provide insights into recognition of the lesion by repair enzymes (*46*, *47*). In this respect, the bulky nature of the lesion suggests that it might be a good substrate for the nucleotide excision repair pathway (*48*). It has been shown in the past that the thermodynamic stabilities of duplex DNA containing the *cis-syn*, (6-4), and Dewar products of TT correlate well with the efficiencies of their removal by *E. coli* (A)BC excinuclease (*45*, *49*). The thermodynamic measurements carried out here suggest that G[8-5]C might be repaired at an efficiency comparable to those of TT photoproducts.

ACKNOWLEDGMENT

We thank Prof. John-Stephen A. Taylor (Washington University) and Prof. John Termini (City of Hope National Medical Center) for providing DNA polymerases.

SUPPORTING INFORMATION AVAILABLE

Michaelis−Menten plots and a plot of $1/T_m$ versus $\ln(C_t/4)$ for undamaged substrates. This material is available free of charge via the Internet at http://pubs.acs.org.

REFERENCES

1. Finkel, T., and Holbrook, N. J. (2000) Oxidants, oxidative stress and the biology of ageing, *Nature 408*, 239−247.
2. Dizdaroglu, M., Jaruga, P., Birincioglu, M., and Rodriguez, H. (2002) Free radical-induced damage to DNA: Mechanisms and measurement, *Free Radical Biol. Med. 32*, 1102−1115.
3. Box, H. C., Budzinski, E. E., Dawidzik, J. D., Wallace, J. C., Evans, M. S., and Gobey, J. S. (1996) Radiation-induced formation of a crosslink between base moieties of deoxyguanosine and thymidine in deoxygenated solutions of d(CpGpTpA), *Radiat. Res. 145*, 641−643.
4. Box, H. C., Budzinski, E. E., Dawidzik, J. B., Gobey, J. S., and Freund, H. G. (1997) Free radical-induced tandem base damage in DNA oligomers, *Free Radical Biol. Med. 23*, 1021−1030.
5. Budzinski, E. E., Dawidzik, J. B., Rajecki, M. J., Wallace, J. C., Schroder, E. A., and Box, H. C. (1997) Isolation and characterization of the products of anoxic irradiation of d(CpGpTpA), *Int. J. Radiat. Biol. 71*, 327−336.
6. Box, H. C., Budzinski, E. E., Dawidzik, J. B., Wallace, J. C., and Iijima, H. (1998) Tandem lesions and other products in X-irradiated DNA oligomers, *Radiat. Res. 149*, 433−439.
7. Romieu, A., Bellon, S., Gasparutto, D., and Cadet, J. (2000) Synthesis and UV photolysis of oligodeoxynucleotides that contain 5-(phenylthiomethyl)-2′-deoxyuridine: A specific photolabile precursor of 5-(2′-deoxyuridilyl)methyl radical, *Org. Lett. 2*, 1085−1088.
8. Box, H. C., Dawidzik, J. B., and Budzinski, E. E. (2001) Free radical-induced double lesions in DNA, *Free Radical Biol. Med. 31*, 856−868.
9. Bellon, S., Ravanat, J. L., Gasparutto, D., and Cadet, J. (2002) Cross-linked thymine-purine base tandem lesions: Synthesis, characterization, and measurement in γ-irradiated isolated DNA, *Chem. Res. Toxicol. 15*, 598−606.
10. Zhang, Q., and Wang, Y. (2003) Independent generation of 5-(2′-deoxycytidinyl)methyl radical and the formation of a novel crosslink lesion between 5-methylcytosine and guanine, *J. Am. Chem. Soc. 125*, 12795−12802.
11. Zhang, Q., and Wang, Y. (2004) Independent generation of the 5-hydroxy-5,6-dihydrothymidin-6-yl radical and its reactivity in dinucleoside monophosphates, *J. Am. Chem. Soc. 126*, 13287−13297.
12. Zeng, Y., and Wang, Y. (2004) Facile formation of an intrastrand cross-link lesion between cytosine and guanine upon Pyrex-filtered UV light irradiation of d(^{Br}CG) and duplex DNA containing 5-bromocytosine, *J. Am. Chem. Soc. 126*, 6552−6553.
13. Gu, C., and Wang, Y. (2004) LC-MS/MS identification and yeast polymerase η bypass of a novel γ-irradiation-induced intrastrand cross-link lesion G[8-5]C, *Biochemistry 43*, 6745−6750.
14. Liu, Z., Gao, Y., and Wang, Y. (2003) Identification and characterization of a novel crosslink lesion in d(CpC) upon 365 nm-irradiation in the presence of 2-methyl-1,4-naphthoquinone, *Nucleic Acids Res. 31*, 5413−5424.

15. Liu, Z., Gao, Y., Zeng, Y., Fang, F., Chi, D., and Wang, Y. (2004) Isolation and characterization of a novel cross-link lesion in d(CpC) induced by one-electron photooxidation, *Photochem. Photobiol. 80*, 209−215.
16. Zhang, Q., and Wang, Y. (2005) Generation of 5-(2′-deoxycytidyl)-methyl radical and the formation of intrastrand cross-link lesions in oligodeoxyribonucleotides, *Nucleic Acids Res. 33*, 1593−1603.
17. Friedberg, E. C., Walker, G. C., and Siede, W. (1995) *DNA Repair and Mutagenesis*, ASM Press, Washington, DC.
18. Echols, H., and Goodman, M. F. (1991) Fidelity mechanisms in DNA replication, *Annu. Rev. Biochem. 60*, 477−511.
19. Kunkel, T. A., and Bebenek, K. (2000) DNA replication fidelity, *Annu. Rev. Biochem. 69*, 497−529.
20. Ito, J., and Braithwaite, D. K. (1991) Compilation and alignment of DNA polymerase sequences, *Nucleic Acids Res. 19*, 4045−4057.
21. Smith, C. A., Baeten, J., and Taylor, J. S. (1998) The ability of a variety of polymerases to synthesize past site-specific cis-syn, trans-syn-II, (6-4), and Dewar photoproducts of thymidylyl-(3′→5′)-thymidine, *J. Biol. Chem. 273*, 21933−21940.
22. Sun, L., Wang, M., Kool, E. T., and Taylor, J. S. (2000) Pyrene nucleotide as a mechanistic probe: Evidence for a transient abasic site-like intermediate in the bypass of dipyrimidine photoproducts by T7 DNA polymerase, *Biochemistry 39*, 14603−14610.
23. Taylor, J. S. (2002) New structural and mechanistic insight into the A-rule and the instructional and non-instructional behavior of DNA photoproducts and other lesions, *Mutat. Res. 510*, 55−70.
24. Wang, Z. (2001) Translesion synthesis by the UmuC family of DNA polymerases, *Mutat. Res. 486*, 59−70.
25. Goodman, M. F. (2002) Error-prone repair DNA polymerases in prokaryotes and eukaryotes, *Annu. Rev. Biochem. 71*, 17−50.
26. Johnson, R. E., Prakash, S., and Prakash, L. (1999) Efficient bypass of a thymine-thymine dimer by yeast DNA polymerase, Polη, *Science 283*, 1001−1004.
27. Masutani, C., Kusumoto, R., Yamada, A., Dohmae, N., Yokoi, M., Yuasa, M., Araki, M., Iwai, S., Takio, K., and Hanaoka, F. (1999) The XPV (xeroderma pigmentosum variant) gene encodes human DNA polymerase η, *Nature 399*, 700−704.
28. Masutani, C., Araki, M., Yamada, A., Kusumoto, R., Nogimori, T., Maekawa, T., Iwai, S., and Hanaoka, F. (1999) Xeroderma pigmentosum variant (XP-V) correcting protein from HeLa cells has a thymine dimer bypass DNA polymerase activity, *EMBO J. 18*, 3491−3501.
29. Johnson, R. E., Haracska, L., Prakash, S., and Prakash, L. (2001) Role of DNA polymerase η in the bypass of a (6-4) TT photoproduct, *Mol. Cell. Biol. 21*, 3558−3563.
30. Patel, S. S., Wong, I., and Johnson, K. A. (1991) Pre-steady-state kinetic analysis of processive DNA replication including complete characterization of an exonuclease-deficient mutant, *Biochemistry 30*, 511−525.
31. Cannistraro, V. J., and Taylor, J. S. (2004) DNA-thumb interactions and processivity of T7 DNA polymerase in comparison to yeast polymerase η, *J. Biol. Chem. 279*, 18288−18295.
32. Valentine, M. R., and Termini, J. (2001) Kinetics of formation of hypoxanthine containing base pairs by HIV-RT: RNA template effects on the base substitution frequencies, *Nucleic Acids Res. 29*, 1191−1199.
33. Goodman, M. F., Creighton, S., Bloom, L. B., and Petruska, J. (1993) Biochemical basis of DNA replication fidelity, *Crit. Rev. Biochem. Mol. Biol. 28*, 83−126.
34. Creighton, S., Bloom, L. B., and Goodman, M. F. (1995) Gel fidelity assay measuring nucleotide misinsertion, exonucleolytic proofreading, and lesion bypass efficiencies, *Methods Enzymol. 262*, 232−256.
35. Breslauer, K. J. (1995) Extracting thermodynamic data from equilibrium melting curves for oligonucleotide order−disorder transitions, *Methods Enzymol. 259*, 221−242.
36. SantaLucia, J., Jr., Kierzek, R., and Turner, D. H. (1991) Functional group substitutions as probes of hydrogen bonding between GA mismatches in RNA internal loops, *J. Am. Chem. Soc. 113*, 4313−4322.
37. Persmark, M., and Guengerich, F. P. (1994) Spectroscopic and thermodynamic characterization of the interaction of N^7-guanyl thioether derivatives of d(TGCTG*CAAG) with potential complements, *Biochemistry 33*, 8662−8672.
38. Einolf, H. J., and Guengerich, F. P. (2000) Kinetic analysis of nucleotide incorporation by mammalian DNA polymerase δ, *J. Biol. Chem. 275*, 16316−16322.
39. Einolf, H. J., and Guengerich, F. P. (2001) Fidelity of nucleotide insertion at 8-oxo-7,8-dihydroguanine by mammalian DNA polymerase δ. Steady-state and pre-steady-state kinetic analysis, *J. Biol. Chem. 276*, 3764−3771.
40. Patel, P. H., and Preston, B. D. (1994) Marked infidelity of human immunodeficiency virus type 1 reverse transcriptase at RNA and DNA template ends, *Proc. Natl. Acad. Sci. U.S.A. 91*, 549−553.
41. Woodside, A. M., and Guengerich, F. P. (2002) Misincorporation and stalling at O^6-methylguanine and O^6-benzylguanine: Evidence for inactive polymerase complexes, *Biochemistry 41*, 1039−1050.
42. Plum, G. E., Grollman, A. P., Johnson, F., and Breslauer, K. J. (1995) Influence of the oxidatively damaged adduct 8-oxodeoxyguanosine on the conformation, energetics, and thermodynamic stability of a DNA duplex, *Biochemistry 34*, 16148−16160.
43. Li, Y., Dutta, S., Doublie, S., Bdour, H. M. d., Taylor, J.-S., and Ellenberger, T. (2004) Nucleotide insertion opposite a cis-syn thymine dimer by a replicative DNA polymerase from bacteriophage T7, *Nat. Struct. Mol. Biol. 11*, 784−790.
44. Iwai, S. (2001) Synthesis and thermodynamic studies of oligonucleotides containing the two isomers of thymine glycol, *Chem.—Eur. J. 7*, 4343−4351.
45. Jing, Y., Kao, J. F., and Taylor, J. S. (1998) Thermodynamic and base-pairing studies of matched and mismatched DNA dodecamer duplexes containing cis-syn, (6-4) and Dewar photoproducts of TT, *Nucleic Acids Res. 26*, 3845−3853.
46. Plum, G. E., and Breslauer, K. J. (1994) DNA lesions. A thermodynamic perspective, *Ann. N.Y. Acad. Sci. 726*, 45−56.
47. Pilch, D. S., Plum, G. E., and Breslauer, K. J. (1995) The thermodynamics of DNA structures that contain lesions or guanine tetrads, *Curr. Opin. Struct. Biol. 5*, 334−342.
48. Sancar, A. (1996) DNA excision repair, *Annu. Rev. Biochem. 65*, 43−81.
49. Svoboda, D. L., Smith, C. A., Taylor, J. S., and Sancar, A. (1993) Effect of sequence, adduct type, and opposing lesions on the binding and repair of ultraviolet photodamage by DNA photolyase and (A)BC excinuclease, *J. Biol. Chem. 268*, 10694−10700.

BI050036+